Supplementary Information for

Enhanced Oxygen Reduction Activity of Platinum Subnanocluster Catalysts through Charge Redistribution

Hironori Tsunoyama[1,†], Akira Ohnuma[2,†], Koki Takahashi[1], Archana Velloth[3], Masahiro Ehara[3], Nobuyuki Ichikuni[4], Masao Tabuchi[5], Atsushi Nakajima[1,*]

1 Department of Chemistry, Faculty of Science and Technology, Keio University, 3-14-1 Hiyoshi, Kohoku-ku, Yokohama, Kanagawa 223-8522, Japan.

2 New Field Pioneering Division, Toyota Boshoku Corp. 1-1 Toyoda-cho, Kariya, Aichi 448-8651, Japan.

3 Department of Theoretical and Computational Molecular Science, Institute for Molecular Science, Myodaiji, Okazaki 444-8585, Japan.

4 Department of Applied Chemistry and Biotechnology, Graduate School of Engineering, Chiba University, 1-33 Yayoi-cho, Inage-ku, Chiba 263-8522, Japan.

5 Synchrotron Radiation Research Center, Nagoya University, Furo-cho, Chikusa, Nagoya 464-8603, Japan.

† Equal contribution.

*Correspondence to: nakajima@chem.keio.ac.jp

Contents

Supplementary text

Materials and methods

Materials

Platinum (Pt) targets (99.9% purity) and the sample of standard Pt/C catalyst (TEC10E50E) were purchased from Tanaka Kikinzoku Kogyo K.K. Rods (ϕ5 mm × 7 mm). Plates (10 × 10 × 0.5 mm) of glassy carbon (GC) were purchased from Ishihara Chemical Co. Ltd. and used after polishing their surfaces with 0.05-μm alumina for at least 3 min. Perchloric acid was purchased from Merck KGaA or Kanto Chemical Co.,Inc. and used as received. Ultrapure water with a resistivity more than 18 MΩ·cm was used for all experiments. High purity gases of oxygen (99.999% purity) and argon (99.9999% purity) were used for electrochemical (EC) measurements. CYTOP® (CTL-109AE) was purchased from AGC Chemical Corporation. A dispersion solution of an ionomer, Nafion (DE2020 CStype, 20wt% in 1-propanol/water), was purchased from FUJIFILM Wako Pure Chemical Corporation.

Methods

Preparation of catalysts

Pt nanocluster (NC) catalysts (Pt_n/GC) were prepared by soft-landing of size-selected NCs utilizing a gas-phase NC generation system (nanojima®-NAP01, Ayabo Corp.)[1, 2] with size selection by a quadrupole mass filter (MAX-16000, Extrel CMS LLC). Single-size NCs were deposited on a polished GC electrode (od. 5 mm × 7 mm) with collision energy less than 1 eV/atom. GC electrodes were polished with 0.05-μm alumina after treatment of a side wall of the electrode with CYTOP® (CTL-10AE), which prevents exposure of the side surface during the deposition and EC measurements. The amount of Pt NCs were quantified by integrating the ion current flowed through the GC electrode and controlled to be below 0.5 ML equivalent based on the number density for the Pt(111) surface. The Pt_n/GC electrodes were kept under an argon atmosphere until just before EC measurements in order to maintain the cleanliness of the surface. For the standard Pt/C catalysts, catalyst coated electrodes were prepared by modifying the reported procedure.[3] The catalyst was first mixed with 80vol% 2-propanol aqueous solution and 1wt% ionomer solution, and then sonicated in an ice bath for 1 h. 10 μL of the catalyst ink was pipetted on a polished GC electrode and subsequently dried in air. The catalyst loading on the electrode was 7.6 $\mu g_{Pt}/cm^2_{GC}$, and the ionomer to carbon ratio was 0.75. For EXAFS measurements, Pt NCs with the density of 0.46 ML equivalent were deposited onto a polished GC plate (10 × 10 mm). Pt NC-decorated GC sample was sealed inside Kapton® or polyethylene films in an argon filled glove box (O_2 conc. <1 vol.ppm) to avoid oxidation of the sample.

Electrochemical measurements

All EC measurements were performed in 0.1 M $HClO_4$ at 30 °C using the reported procedure.[4] The working electrode (WE) was the Pt_n/GC electrodes. A reversible hydrogen electrode (RHE) was used as the reference electrode (RE) and the same set-up: platinized Pt with a hydrogen reservoir, was used as the counter electrode (CE) as well. Both CE and RE electrodes were separated from a WE-compartment by porous Vycor® glass. To avoid disturbance by trace amount of impurities, the glassware and accessories were boiled three times in water for more than 5 min. and then carefully rinsed with ultrapure water with a resistivity more than 18 MΩ·cm. Cyclic voltammograms (CVs) were measured between 0.05 – 1.2 V at a scan rate of 50 $mV \cdot s^{-1}$ in the argon-saturated solution. The ORR activity was then measured by recording a linear sweep, hydrodynamic voltammogram at a scan rate of 50 $mV \cdot s^{-1}$ with the electrode rotation of 400 rpm with the rotating disk electrode (RDE) method after the

solution was saturated with oxygen. The kinetic limiting current density was calculated by using the Koutecky-Levich equation as reported by Yamamoto and co-workers.[5, 6]

XAFS measurements

Pt L_3-edge EXAFS measurements were performed using the BL5S1 beamline at Aichi Synchrotron Radiation Center (Proposal No. 201804105 and 201805103) and the BL12C in Photon Factory (KEK, Proposal No. 2019G041). Incident x-rays were monochromatized by a Si(111) double crystal monochromator and focused by Rh coated mirrors. Typical beam size was 0.5 × 0.5 mm. The sample of Pt_6/GC was mounted 20 – 45º from the incident light. Partial fluorescence yield for the Pt $L\alpha$ line was measured by seven silicon drift detectors placed 90º from the incident light. All EXAFS profiles were measured at room temperature. The x-ray energy was calibrated with the edge jump for Pt L_3-edge of a Pt foil. Analyses of EXAFS profiles were conducted by using the Athena program.[7] The $\chi(k)$ spectra were extracted after subtraction of atomic absorption background using a cubic spline function followed by normalization at the edge jump. The k^2-weighted $\chi(k)$ spectra were used for further analyses. The experimental $\chi(k)$ spectra were simulated by using the FEFF6 code[8] incorporated in the Demeter system[7] along with the Larch library[9] based on equilibrium geometries for Pt_6/Graphene (Gr) obtained by DFT calculations. In the fitting procedures, energy shift (E_0: –10 to +10 eV) and distance shift (ΔR: +0.10 to –0.10 Å) values were first adjusted to reproduce the period of the $\chi(k)$ spectra. Finally, at the optimum E_0 and ΔR conditions, Debye-Waller factor (σ^2) and amplitude (S_0) were adjusted to achieve better agreement based on a R^2 value.

Density functional theory calculations

The Pt_6 supported on single-layer-graphene surface model were examined by using plane-wave-based DFT calculations. Spin polarized DFT calculations were performed using the Vienna Ab initio Simulation Package (VASP version 5.4.1).[10, 11] The projector-augmented wave (PAW)[12, 13] with a generalized gradient approximation (GGA) refined by Perdew, Burke and Ernzerhof (PBE)[14] was used. The calculations were performed using a 6 x 6 graphene supercell (72 atoms) with periodic bound conditions and the periodic images were separated by 15 Å of vacuum to prevent image interactions. A kinetic energy cutoff of 400 eV was used and the Brillouin zone was sampled using a 3 x 3 x 1 Γ centered *k*-point mesh. Gaussian broadening method with a smearing width of 0.05 eV was used to improve convergence of states near the Fermi level. The convergence parameters for the electronic structure and geometry optimization were set as 1×10^{-5} eV/cell and 5×10^{-3} eV/Å for energy and force respectively. Structures were fully relaxed during the geometry optimization and the possible initial structures of Pt_6 cluster were examined. Charge analysis was performed by Bader charge analysis 1.02 program developed by Henkelman group.[15]

First, we examined the stable structures of free Pt_6 clusters whose local minima are shown in Figure S1 with their relative energies. Among these eight 2D or 3D local minimum structures (**1'** – **8'**), the most stable structure was the planar structure, which is consistent with the previous study.[16] Based on these structures, we examined possible adsorption structures on graphene with all the geometrical parameters fully optimized. Although the 2D structure was energetically most favourable, the 3D structure was more strongly bound on the pristine graphene in view of adsorption energy as listed in Table S1.

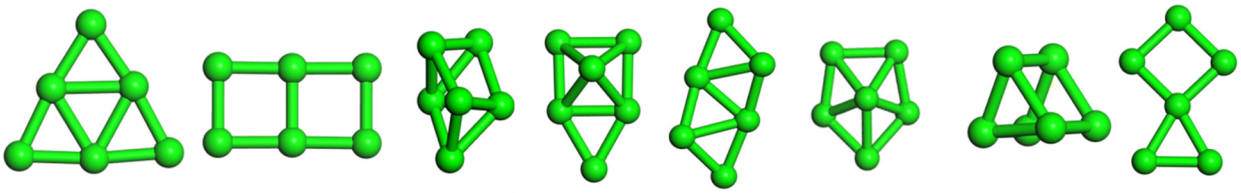

Pt_6 (1′)	Pt_6 (2′)	Pt_6 (3′)	Pt_6 (4′)	Pt_6 (5′)	Pt_6 (6′)	Pt_6 (7′)	Pt_6 (8′)
0.000	0.230	0.667	0.739	0.863	0.894	0.962	1.287

Figure S1. Optimized structures for free Pt_6 isomers **1'** – **8'**. Relative energies in eV are also indicated relative to the most stable isomer **1'**.

Table S1. Adsorption energies, average Pt-C bond lengths ($d_{Pt\text{-}C}$) and average Pt-Pt ($d_{Pt\text{-}Pt}$) bond lengths for Pt_6 adsorbed on PG.

Pt_6/Gr	**Adsorption energy (eV)**	**$d_{Pt\text{-}C}$ (Å)**	**$d_{Pt\text{-}Pt}$ (Å)**
Pt_6 (**1**)	-2.334	2.286	2.521
Pt_6 (**2**)	-2.111		2.519
Pt_6 (**3**)	-2.443	2.251	2.504
Pt_6 (**4**)	-2.544	2.245	2.499
Pt_6 (**5**)	-2.544	2.209	2.499
Pt_6 (**6**)	-2.490	2.232	2.503
Pt_6 (7)	**-2.480**	**2.165**	**2.585**

Transmission electron microscopy (TEM)

High resolution TEM images were recorded at the Research Center for Ultra-High Voltage Electron Microscopy, Osaka University using a spherical aberration corrected high-angle annular dark field scanning transmission electron microscope (HAADF-STEM, JEM-ARM200F, JEOL Ltd.) with an acceleration voltage of 200 kV (Project No. A-18-OS-0017). Single-size Pt NCs were deposited on an amorphous carbon coated copper grid (thickness of carbon coating ~ 20 nm) by soft-landing of size-selected NCs generated with nanojima®. Although Pt_6 sub-NCs are deposited on an amorphous carbon instead of a glassy-carbon, the TEM image exhibits some ~0.5 nm spots, which seems consistent with individual Pt_6 sub-NCs immobilized on a surface.

Supplementary figures

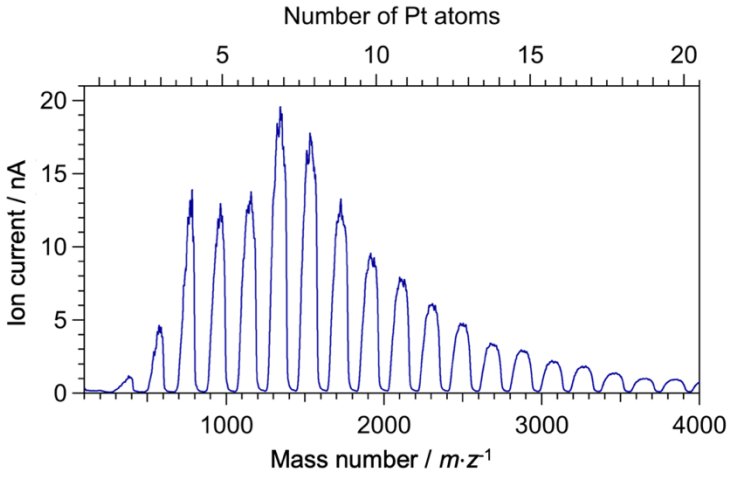

Figure S2. A representative mass spectrum of Pt nanocluster anions (Pt_n^-; n = 2 - 20) generated with nanojima®.

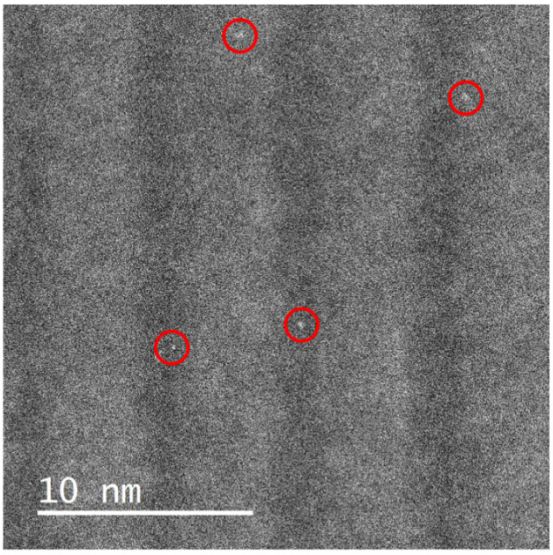

Figure S3. HAADF-STEM image of Pt_6 sub-NCs deposited on an amorphous carbon coated copper grid. Red circles indicate individual Pt_6 sub-NCs.

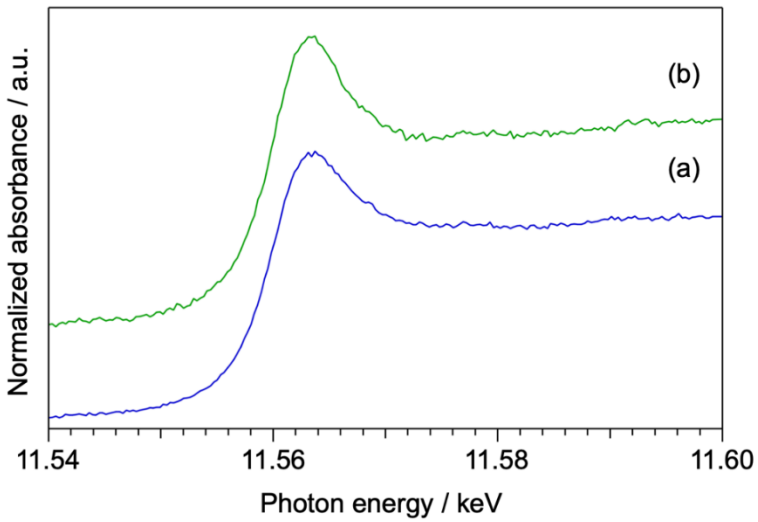

Figure S4. Pt L_3-edge x-ray absorption near edge structure (XANES) spectra for (a) Pt_6/GC under argon and (b) Pt_6/GC under air. The spectra were normalized at the edge jump, and have been offset vertically for clarity of presentation.

Table S2. Summary of EXAFS fitting results for Pt_6/GC and Pt foil.

Shell	CN[a]	Distance /Å	σ^2 / Å^2 [b]	ΔE / eV[c]	R factor[d]
			Pt_6/GC		
Pt-Pt[e]	7.10 (100)	2.738	0.0069 (9)	6.43 (208)	0.012
Pt-Pt[f]	4.25 (43)[g]	2.732	0.0036[h]	5.83 (401)	0.044
			Pt foil		
Pt-Pt[i]	10.1 (4)	2.770	0.0047 (2)	8.91 (52)	0.0005
Pt-Pt[j]	10.7 (4)	2.764	0.0051 (1)	7.34 (49)	0.0027

[a] Coordination number, [b] Debye-Waller factor, [c] Energy difference in the absorption threshold, [d] R factor by k^3 weight, [e] fitting ranges for k: 5 – 12 Å^{-1} and r: 1.56 – 3.28 Å, [f] fitting ranges for k: 5 – 12 Å^{-1} and r: 1.56 – 3.28 Å with the fixed σ^2 value used for estimating statistical disordering effect on the bond distances of Pt_6, [g] smaller CN was obtained after reduction of DW factor with the reasonable value, which is almost consistent with CN for isomer 7 of Pt_6/Gr (fig. 3), [h] fixed value was used in the fitting, [i] fitting ranges for k: 5 – 12 Å^{-1} and r: 1.60 – 3.38 Å, [j] fitting ranges for k: 3 – 16 Å^{-1} and r: 1.50 – 3.34 Å.

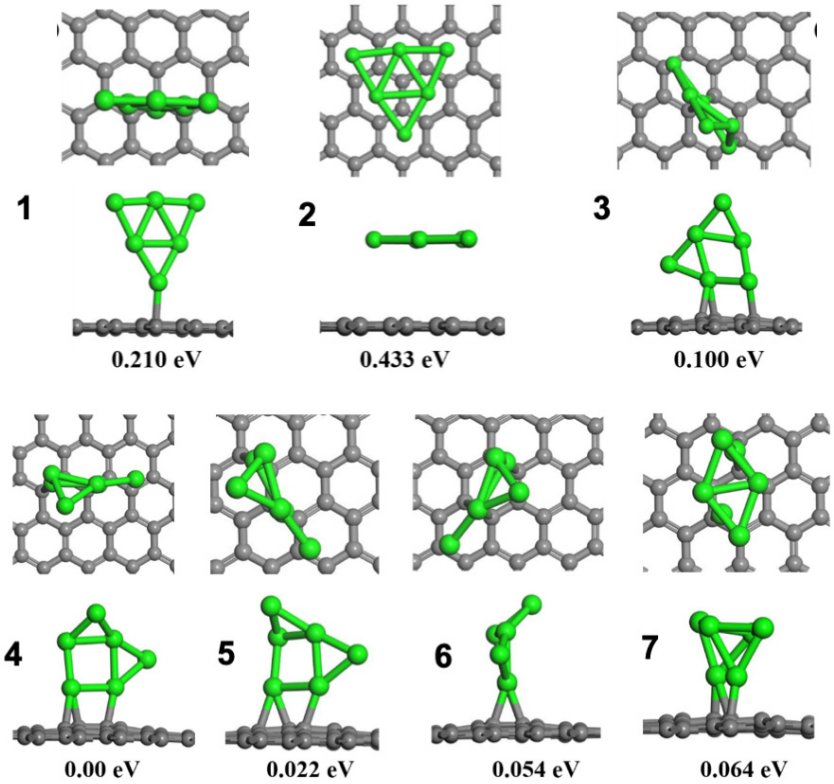

Figure S5. Optimized isomeric structures for Pt_6/Gr isomers **1** - **7**. Relative energies in eV are also indicated relative to the most stable isomer **4**. Isomer **7** represents the most probable structure candidate.

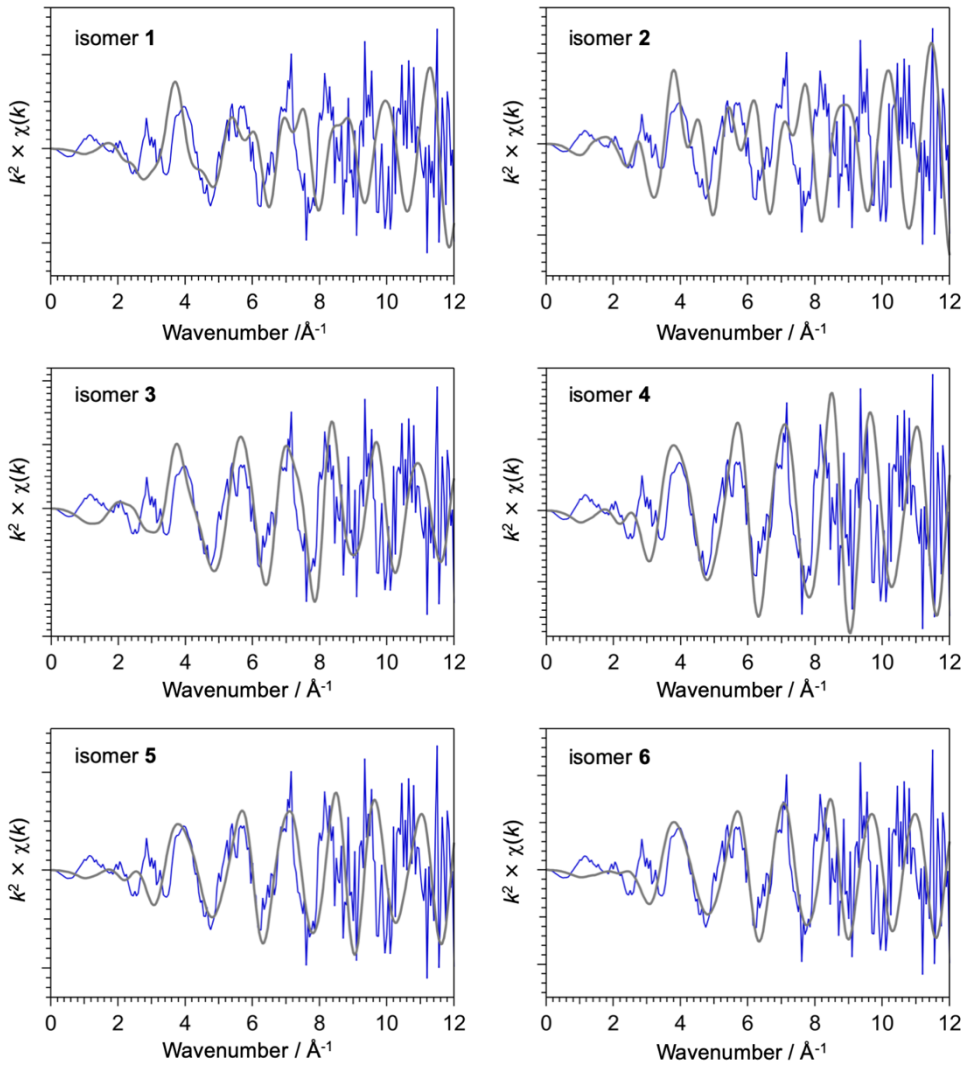

Figure S6. FEFF simulations of $\chi(k)$ spectra for all other isomers of Pt_6/Gr except for isomer **7** shown in Fig. 2c of the main text. Blue and black curves represent experimental and simulated $\chi(k)$ spectra, respectively. Pt_6/Gr coordinates were used without scaling of the geometry.

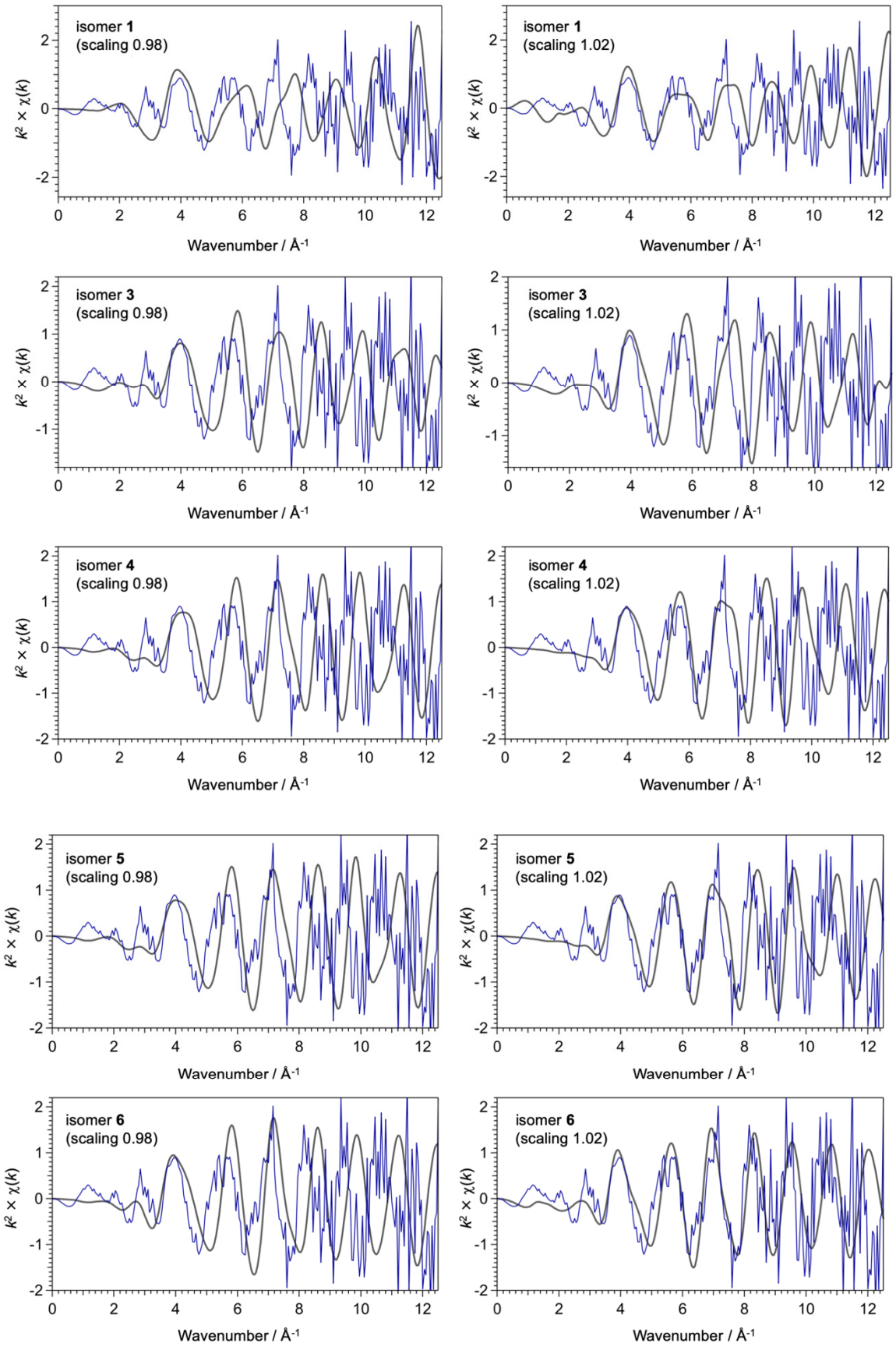

Figure S7. FEFF simulations with scaling of the coordinates for Pt_6/Gr isomers **1**, **3**, **4**, **5** and **6** (0.98 or 1.02). Isomer **2** was excluded because of large deviations of the oscillation behavior. Blue and black curves represent experimental and simulated $\chi(k)$ spectra, respectively.

References

1. H. Tsunoyama, C. Zhang, H. Akatsuka, H. Sekiya, T. Nagase and A. Nakajima, *Chem. Lett.*, 2013, **42**, 857-859.
2. H. Tsunoyama, M. Shibuta, M. Nakaya, T. Eguchi and A. Nakajima, *Acc. Chem. Res.*, 2018, **51**, 1735-1745.
3. S. S. Kocha, K. Shinozaki, J. W. Zack, D. J. Myers, N. N. Kariuki, T. Nowicki, V. Stamenkovic, Y. Kang, D. Li and D. Papageorgopoulos, *Electroanal.*, 2017, **8**, 366-374.
4. T. Nagai, H. Murata and Y. Morimoto, *ECS Trans.*, 2012, **50**, 1539-1545.
5. T. Imaoka, H. Kitazawa, W.-J. Chun and K. Yamamoto, *Angew. Chem. Int. Ed. Engl.*, 2015, **54**, 9810-9815.
6. K. Yamamoto, T. Imaoka, W.-J. Chun, O. Enoki, H. Katoh, M. Takenaga and A. Sonoi, *Nat. Chem.*, 2009, **1**, 397-403.
7. B. Ravel and M. Newville, *J. Synchrotron Radiat.*, 2005, **12**, 537-541.
8. S. I. Zabinsky, J. J. Rehr, A. Ankudinov, R. C. Albers and M. J. Eller, *Phys. Rev. B: Condens. Matter Mater. Phys.*, 1995, **52**, 2995-3009.
9. M. Newville, *J. Phys.: Conf. Series*, 2013, **430**, 012007.
10. G. Kresse and J. Hafner, *Phys. Rev. B: Condens. Matter Mater. Phys.*, 1993, **47**, 558-561.
11. G. Kresse and J. Hafner, *Phys. Rev. B: Condens. Matter Mater. Phys.*, 1994, **49**, 14251-14269.
12. P. E. Blöchl, *Phys. Rev. B,* 1994, **50**, 17953.
13. G. Kreese and D. Joubert, *Phys. Rev. B,* 1999, **59**, 1758.
14. J. P. Perdew, K. Burke and M. Ernzerhof, *Phys. Rev. Lett.,* 1996, **77**, 3865.
15. G. Henkelman, A. Arnaldsson and H. Jónsson, *Comput. Mater. Sci.,* 2006, **36**, 354‑360.
16. C. R. C. Rêgo, P. Tereshchuk, L. N. Oliveira and J. L. F. Da Silva, *Phy. Rev. B.,* 2017, **95**, 235422.